Séminaire Lotharingien de Combinatoire **XX** (2026)
Article #26, 12 pp.

Proceedings of the 38th Conference on Formal Power Series and Algebraic Combinatorics (Seattle)

Cylindric growth diagrams

Sergi Elizalde*

Department of Mathematics, Dartmouth College, Hanover, NH 03755

Abstract. Semistandard cylindric tableaux were introduced by Gessel and Krattenthaler, and later studied by Postnikov in connection to Gromov–Witten invariants. A cylindric analogue of the Robinson–Schensted–Knuth (RSK) correspondence was discovered by Neyman, who described it in terms of an insertion operation adapted from a construction for skew tableaux due to Sagan and Stanley.

In this abstract we introduce a cylindric version of Fomin's growth diagrams, and use it to provide an alternative description of the cylindric RSK correspondence. This natural description elucidates the symmetry obtained when switching the insertion and recording tableaux. Our construction also shows that, in the special case where these two tableaux are equal and standard (i.e., each entry appears once), cylindric RSK is equivalent to a bijection of Courtiel, Elvey Price and Marcovici for certain walks in simplicial regions. We introduce oscillating cylindric tableaux and use them to encode such walks.

Keywords: growth diagram, cylindric tableau, RSK, differential poset

1 Introduction

The main goal of this extended abstract is to introduce a cylindric analogue of Fomin's growth diagrams, where the role of Young tableaux is played by cylindric tableaux.

Semistandard cylindric tableaux were defined by Postnikov in [13], although they can be viewed as a special case of what Gessel and Krattenthaler called cylindric partitions in [6], which are plane partitions with additional constraints between the entries of the first and last rows. Postnikov showed that semistandard cylindric tableaux are related to the structure constants of the quantum cohomology ring of the Grassmannian, called the 3-point Gromov–Witten invariants. Specifically, he showed that these coefficients appear when expanding the generating functions for semistandard cylindric tableaux of a given shape (later called cylindric skew Schur functions in [10]) in terms of ordinary Schur functions.

On the other hand, growth diagrams were first introduced by Fomin [4, 5] in order to generalize the Robinson–Schensted (RS) correspondence [18], a celebrated bijection between permutations and pairs of standard Young tableaux of the same shape. Over

*sergi.elizalde@dartmouth.edu. Partially supported by Simons Collaboration Grant #929653.

the years, growth diagrams have proved to be very useful in various settings (see e.g. [8]), and they have been extended [14, Ch. 4] in order to provide an alternative description of the more general Robinson–Schensted–Knuth (RSK) correspondence, a bijection between matrices with non-negative integer entries and pairs of semistandard Young tableaux of the same shape. Growth diagrams are built in terms of local rules which describe how to label the vertices of a certain grid by elements of a differential poset [17]. In the basic case, this is the poset of partitions ordered by containment of their shapes, known as Young's lattice. Even though the lattice of cylindric shapes ordered by containment is no longer a differential poset (it does not have a minimum element), we will show that this lattice can still be used to define a cylindric analogue of growth diagrams.

Cylindric growth diagrams, as we call them, have several applications. First, they provide a natural description of Neyman's cylindric analogue of the RSK correspondence [12], which was originally defined in terms of an insertion operation inspired in Sagan and Stanley's insertion on skew tableaux [16]. In particular, our description using cylindric growth diagrams elucidates the symmetry of the correspondence, similarly to how Fomin's original growth diagrams explain the symmetry of the classical RS correspondence.

Second, cylindric growth diagrams, in the symmetric case and when restricted to standard cylindric tableaux (i.e., where each entry appears once), provide the "right" setting to understand a bijection of Courtiel et al. [2] for certain simplicial walks with a given starting point and an arbitrary pattern of forward and backward steps. Compared to the ad-hoc description from [2], which is based on a "convergent rewriting system" and then rephrased in terms of tilings of square using a certain set of tiles, our description arises naturally once we interpret the walks as oscillating cylindric tableaux. In particular, the local rules of the cylindric growth diagrams determine the set of available tiles.

This extended abstract is organized as follows. In Section 2, we give some background on cylindric tableaux and on the cylindric RSK correspondence, described by Neyman [12] in terms of insertion operations. In Section 3, we introduce the notion of cylindric growth diagrams and use them to give an alternative description of cylindric RSK. In the standard case, the forward and backward rules for cylindric growth diagrams resemble the classical ones, except that the row indices are periodic and that no cells can be filled with crosses. In the semistandard case, our general construction is vaguely reminiscent of a description by Berenstein and Kirillov [1] of a variant of RSK (as a bijection between matrices of nonnegative integers and plane partitions) in terms of piecewise linear transformations. In Section 4, we introduce cylindric oscillating tableaux, and we use them to construct a bijection for simplicial walks with a given starting point and an arbitrary pattern of forward and backward steps.

2 The cylindric RSK correspondence

For positive integers d and ℓ, define the cylinder $\mathcal{C}_{d,\ell} = \mathbb{Z}^2/(-d,\ell)\mathbb{Z}^2$. Elements of $\mathcal{C}_{d,\ell}$, called cells, are equivalence classes $\langle i,j\rangle = (i,j) + (-d,\ell)\mathbb{Z}^2$, where $i,j \in \mathbb{Z}$. As in [13, 12], we draw points $(i,j) \in \mathbb{Z}^2$ as unit squares with vertices $(i-1,j-1), (i-1,j)$, $(i,j-1), (i,j)$, where the positive x-axis points downward and the positive y-axis points to the right, to be consistent with the English notation for Young diagrams. With this notation, (i,j) represents the square in row i and column j, where row indices increase from top to bottom, and column indices increase from left to right.

A *cylindric shape of period* (d,ℓ) is a doubly infinite weakly decreasing sequence of integers, $\lambda = (\lambda_i)_{i\in\mathbb{Z}}$, such that $\lambda_i = \lambda_{i+d} + \ell$ for all $i \in \mathbb{Z}$. A cylindric shape is determined by any integers $\lambda_1,\ldots,\lambda_d$ satisfying $\lambda_d + \ell \geq \lambda_1 \geq \lambda_2 \geq \cdots \geq \lambda_d$. We will write $\lambda = [\lambda_1,\lambda_2,\ldots,\lambda_d]$ or $\lambda = [\lambda_1\lambda_2\ldots\lambda_d]$. Denote by $\Lambda_{d,\ell}$ the set of cylindric shapes of period (d,ℓ). For $\lambda \in \Lambda_{d,\ell}$, the region $\{(i,j) \in \mathbb{Z}^2 : j \leq \lambda_i\}$ is a union of equivalence classes, which we denote by $Y_\lambda = \{\langle i,j\rangle \in \mathcal{C}_{d,\ell} : j \leq \lambda_i\}$, and we call it the Young diagram of λ. We often identify λ with Y_λ when we talk about adding or removing cells to λ.

Consider the partial order on $\Lambda_{d,\ell}$ defined by containment of their Young diagrams: given $\lambda,\mu \in \Lambda_{d,\ell}$, write $\mu \subseteq \lambda$ if $Y_\mu \subseteq Y_\lambda$; equivalently, if $\mu_i \leq \lambda_i$ for all $i \in \mathbb{Z}$. For $\mu \subseteq \lambda$, the *cylindric Young diagram of shape* λ/μ is the finite set $Y_{\lambda/\mu} = Y_\lambda \setminus Y_\mu = \{\langle i,j\rangle \in \mathcal{C}_{d,\ell} : \mu_i < j \leq \lambda_i\}$. We denote its cardinality by $|\lambda/\mu| = \sum_{i=1}^d (\lambda_i - \mu_i)$. We also define $|\lambda| = \lambda_1 + \cdots + \lambda_d$, which may be negative.

A *semistandard cylindric tableau* of shape λ/μ is a function $T : Y_{\lambda/\mu} \to \{1,2,3,\ldots\}$ such that $T(\langle i,j\rangle) \leq T(\langle i+1,j\rangle)$ and $T(\langle i,j\rangle) < T(\langle i,j+1\rangle)$ for all i,j; equivalently, a filling of the cells in $Y_{\lambda/\mu}$ so that entries are weakly increasing along rows (from left to right) and strictly increasing along columns (from top to bottom). Such a tableau is *standard* if it is filled with the entries $1,2,\ldots,|\lambda/\mu|$, each appearing exactly once. For example, the semistandard cylindric tableau T on the top left of Figure 2 has shape α/μ, where $\alpha = [5,5,3]$ and $\mu = [2,1,0]$ are cylindric shapes in $\Lambda_{3,4}$; here $|\alpha/\mu| = 10$. The four cylindric tableaux in Figure 1 are standard.

Denote by $\mathrm{SSCT}_{d,\ell}(\lambda/\mu)$ (resp. $\mathrm{SCT}_{d,\ell}(\lambda/\mu)$) the set of semistandard (resp. standard) cylindric tableaux of period (d,ℓ) and shape λ/μ. If $T \in \mathrm{SSCT}_{d,\ell}(\lambda/\mu)$, we call λ and μ the outer shape and the inner shape of T, respectively. Define the weight $\mathrm{wt}(T) = \prod_i x_i^{c_i}$, where c_i is the number of times that the entry i appears in T. For example, if $T \in \mathrm{SSCT}_{3,4}([5,5,3]/[2,1,0])$ is the tableau from Figure 2, then $\mathrm{wt}(T) = x_1^4 x_2^2 x_3 x_4^3$. Denote by $\mathrm{SSCT}^n_{d,\ell}(\cdot/\mu)$ (respectively, $\mathrm{SSCT}^n_{d,\ell}(\lambda/\cdot)$) the set of semistandard cylindric tableaux with n cells and inner shape μ (respectively, outer shape λ), and define analogous notation for SCT.

We will call λ/μ a *horizontal strip* if the cylindric Young diagram $Y_{\lambda/\mu}$ contains at most one cell in each column; equivalently, if $\mu_i \leq \lambda_i \leq \mu_{i-1}$ for all i. In any semistandard cylindric tableau, the set of cells containing a given number form a horizontal strip.

For $\lambda, \mu \in \Lambda_{d,\ell}$ with $\mu \subseteq \lambda$ and $|\lambda/\mu| = n$, elements of $\mathrm{SCT}_{d,\ell}(\lambda/\mu)$ are in bijection with sequences of shapes $\mu = \lambda^{(0)} \subset \lambda^{(1)} \subset \cdots \subset \lambda^{(n)} = \lambda$, where $\lambda^{(k)} \in \Lambda_{d,\ell}$ for all k, and each $\lambda^{(k)}$, for $1 \leq k \leq n$, is obtained from $\lambda^{(k-1)}$ by adding a cell. Similarly, elements of $\mathrm{SSCT}_{d,\ell}(\lambda/\mu)$ with entries $\leq N$ are in bijection with sequences of shapes $\mu = \lambda^{(0)} \subseteq \lambda^{(1)} \subseteq \cdots \subseteq \lambda^{(N)} = \lambda$, where $\lambda^{(k)} \in \Lambda_{d,\ell}$ for all k, and $\lambda^{(k)}/\lambda^{(k-1)}$ is a horizontal strip for each $1 \leq k \leq N$. For $T \in \mathrm{SSCT}_{d,\ell}(\lambda/\mu)$, we denote this sequence by

$$\mathrm{ssh}(T) = (\lambda^{(0)}, \lambda^{(1)}, \dots), \tag{2.1}$$

where $\lambda^{(k)}$ is the outer shape of the tableau consisting of the cells of T with entries $\leq k$.

In [16], Sagan and Stanley introduced analogues of the RSK correspondence for skew tableaux. Neyman later adapted these algorithms to semistandard cylindric tableaux in [12], describing a bijection from pairs of cylindric tableaux with given outer shapes to pairs of cylindric tableaux with given inner shapes. The *cylindric RSK* correspondence, denoted by CRSK, relies on a row insertion operation which, in its simplest version, removes an inner corner of a tableau and inserts the removed entry into the next row. This entry may in turn bump a larger entry into the following row. This process is repeated until the bumped entry becomes the largest entry in the row where it is inserted. Unlike in the usual RSK correspondence, this process may visit the same row multiple times, since rows are indexed modulo d. To deal with repeated entries in semistandard cylindric tableaux, a more complicated multi-insertion operation is described in [12].

Theorem 1 ([12]). *Fix $\alpha, \beta \in \Lambda_{d,\ell}$. There is a bijection*

$$\mathrm{CRSK} : \bigsqcup_{\mu \subseteq \alpha,\beta} \mathrm{SSCT}_{d,\ell}(\alpha/\mu) \times \mathrm{SSCT}_{d,\ell}(\beta/\mu) \to \bigsqcup_{\lambda \supseteq \alpha,\beta} \mathrm{SSCT}_{d,\ell}(\lambda/\beta) \times \mathrm{SSCT}_{d,\ell}(\lambda/\alpha)$$

such that, if $\mathrm{CRSK}(T, U) = (P, Q)$, *then* $\mathrm{wt}(T) = \mathrm{wt}(P)$ *and* $\mathrm{wt}(U) = \mathrm{wt}(Q)$.

When restricted to standard cylindric tableaux, that is, when $\mathrm{wt}(T) = \mathrm{wt}(P) = x_1 \dots x_n$ and $\mathrm{wt}(U) = \mathrm{wt}(Q) = x_1 \dots x_m$, we denote this bijection by

$$\mathrm{CRS} : \bigsqcup_{\mu \subseteq \alpha,\beta} \mathrm{SCT}_{d,\ell}(\alpha/\mu) \times \mathrm{SCT}_{d,\ell}(\beta/\mu) \to \bigsqcup_{\lambda \supseteq \alpha,\beta} \mathrm{SCT}_{d,\ell}(\lambda/\beta) \times \mathrm{SCT}_{d,\ell}(\lambda/\alpha). \tag{2.2}$$

Note that $|\alpha/\mu| = |\lambda/\beta| = n$ and $|\beta/\mu| = |\lambda/\alpha| = m$ in this case.

3 Cylindric growth diagrams

Growth diagrams were introduced by Fomin [4, 5] as an alternative description of the RS correspondence, in order to generalize it to differential posets [17]. We refer the reader to

[18, Sec. 7.13] and [15, Sec. 5.2] for expositions on growth diagrams. Roby showed in [14, Ch. 3] that Sagan and Stanley's analogue of the RSK algorithm for skew tableaux [16] also has a natural description in terms of growth diagrams.

In this section we extend the growth diagram approach to the cylindric case, providing a new description of the cylindric RSK correspondence from Theorem 1. This description makes the construction more natural, and it elucidates the symmetry obtained when switching the two tableaux in the pair.

3.1 Growth diagrams for SCT

We start with the case of standard cylindric tableaux, which is simpler and more similar to the classical case. In Subsection 3.2 we will explain how to deal with repeated entries.

Fix $\alpha, \beta \in \Lambda_{d,\ell}$ and $n, m \geq 0$. Let $T \in \mathrm{SCT}_{d,\ell}(\alpha/\mu)$ and $U \in \mathrm{SCT}_{d,\ell}(\beta/\mu)$, where $\mu \subseteq \alpha, \beta$ satisfies $|\alpha/\mu| = n$ and $|\beta/\mu| = m$. We will construct a cylindric growth diagram to compute the pair $(P, Q) = \mathrm{CRS}(T, U)$. We draw the growth diagram as an $m \times n$ rectangular grid whose vertices have integer coordinates (x, y) for $0 \leq x \leq m$ and $0 \leq y \leq n$. (Here we use the usual orientation of the axes, rather than the rotated convention that we used for cells of the cylinder $\mathcal{C}_{d,\ell}$ in Section 2.) Each vertex of the grid will be labeled with an element of $\Lambda_{d,\ell}$.

Before we proceed with the description of the labels, let us highlight some differences between our approach and the usual setup for growth diagrams [14, 15, 18]. Unlike Young's lattice, the poset $(\Lambda_{d,\ell}, \subseteq)$ of cylindric shapes ordered by containment is not an *r-differential poset* as defined in [17, Def. 1.1], since it does not have a minimal element. However, if we disregard this condition and relax the usual requirement that r be positive, then $(\Lambda_{d,\ell}, \subseteq)$ satisfies the other parts of this definition with $r = 0$. Specifically,

(D1) it is locally finite and it has a rank function (letting the rank of ρ be $|\rho|$, as defined in Section 2);

(D2) for any $\rho, \nu \in \Lambda_{d,\ell}$ with $\rho \neq \nu$, the number of elements covered by both ρ and ν equals the number of elements that cover both ρ and ν (this number is always 0 or 1); and

(D3) every $\rho \in \Lambda_{d,\ell}$ covers the same number of elements that it is covered by (this number equals $c(\rho) = |\{i \in \{1, 2, \ldots, d\} : \rho_{i-1} > \rho_i\}|$).

For comparison, condition (D3) for an r-differential poset states that if an element covers exactly k elements (for some k), then it must be covered by exactly $k + r$ elements. One consequence of setting $r = 0$ in this condition is that, unlike usual growth diagrams, cylindric growth diagrams will never have crosses in the squares of the $m \times n$ grid. Another difference is that, for any edge in a cylindric growth diagram for SCT with endpoints labeled ν and ρ, with ρ above or to the right of ν, the shape ρ is obtained from ν by adding exactly one cell; in particular, $\nu \neq \rho$.

Now we are ready to describe the labels of the vertices of the $m \times n$ grid. We start by labeling the vertices in the left boundary (i.e., those with coordinates of the form $(0, y)$), from bottom to top, by the sequence $\mathrm{ssh}(T)$, as defined in equation (2.1). Similarly, we label the vertices in the bottom boundary (i.e., those of the form $(x, 0)$), from left to right, by the sequence $\mathrm{ssh}(U)$. In particular, vertex $(0,0)$ has label μ, vertex $(0, n)$ has label α, and vertex $(m, 0)$ has label β. See Figure 1 for an example.

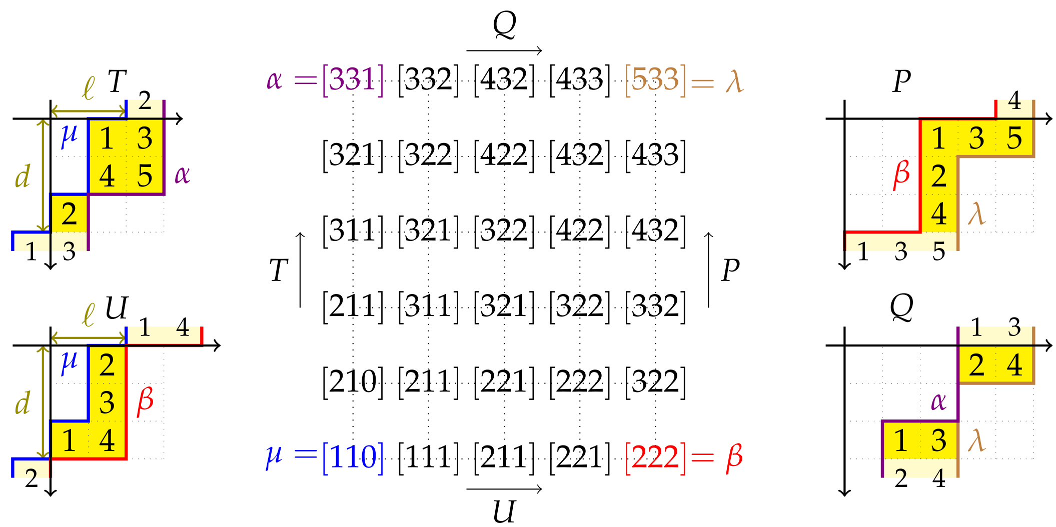

Figure 1: The computation of $\mathrm{CRS}(T, U) = (P, Q)$ using growth diagrams.

To compute the labels of the remaining vertices, we use the following *forward local rule*, which describes, for each unit square of the grid, the label of the upper-right vertex in terms of the labels of the other three vertices. Let the diagram below denote the labels of the vertices of a unit square, and suppose that $\rho^{\llcorner}$, $\rho^{\ulcorner}$ and $\rho^{\lrcorner}$ have already been computed.

$$\begin{array}{cc} \rho^{\ulcorner} & \rho^{\urcorner} \\ \rho^{\llcorner} & \rho^{\lrcorner} \end{array} \tag{3.1}$$

Then $\rho^{\urcorner}$ is computed as follows:

(F1) If $\rho^{\ulcorner} \neq \rho^{\lrcorner}$, let $\rho^{\urcorner} = \rho^{\ulcorner} \cup \rho^{\lrcorner}$, i.e., $\rho^{\urcorner}_i = \max\{\rho^{\ulcorner}_i, \rho^{\lrcorner}_i\}$ for all i.

(F2) If $\rho^{\ulcorner} = \rho^{\lrcorner}$, then this shape is obtained from $\rho^{\llcorner}$ by adding a cell to some row i. Let $\rho^{\urcorner}$ be the shape obtained from $\rho^{\ulcorner} = \rho^{\lrcorner}$ by adding a cell to row $i+1$ (with indices modulo d).

Once all the labels of the $m \times n$ grid have been computed, let λ be the label of vertex (m, n), and note that $|\lambda/\beta| = n$ and $|\lambda/\alpha| = m$. Let $P \in \mathrm{SCT}_{d,\ell}(\lambda/\beta)$ be such that $\mathrm{ssh}(P)$ is the sequence of the labels of the right boundary of the grid (i.e., vertices of the form (m, y)), from bottom to top. Similarly, let $Q \in \mathrm{SCT}_{d,\ell}(\lambda/\alpha)$ be such that $\mathrm{ssh}(Q)$ is the sequence of labels of the top boundary (i.e., the vertices of the form (x, n)), from left to right.

It can be shown that the pair of tableaux (P, Q) obtained in this way is precisely the image of (T, U) under the map CRS from equation (2.2), which is described in [12] in terms of iterated insertion operations.

The forward local rule can be inverted in order to determine the label of the lower-left vertex of a unit square of the grid in terms of the labels of the other three vertices. Assuming that $\rho^{\ulcorner}$, $\rho^{\lrcorner}$ and $\rho^{\urcorner}$ have already been computed, the following *backward local rule* determines $\rho^{\llcorner}$:

(B1) If $\rho^{\ulcorner} \neq \rho^{\lrcorner}$, let $\rho^{\llcorner} = \rho^{\ulcorner} \cap \rho^{\lrcorner}$, i.e., $\rho^{\urcorner}_i = \min\{\rho^{\ulcorner}_i, \rho^{\lrcorner}_i\}$ for all i.

(B2) If $\rho^{\ulcorner} = \rho^{\lrcorner}$, then this shape is obtained from $\rho^{\urcorner}$ by removing a cell from some row $i + 1$. Let $\rho^{\llcorner}$ be the shape obtained from $\rho^{\ulcorner} = \rho^{\lrcorner}$ by removing a cell from row i (with indices modulo d).

This allows us to compute the map CRS^{-1} that recovers the pair (T, U) from the pair $(P, Q) \in \mathrm{SCT}_{d,\ell}(\lambda/\beta) \times \mathrm{SCT}_{d,\ell}(\lambda/\alpha)$.

3.2 Growth diagrams for SSCT

Next we generalize the above construction to deal with semistandard cylindric tableaux. In this case, for any edge of the cylindric growth diagram with endpoints labeled ν and ρ, with ρ above or to the right of ν, the shape ρ/ν is a horizontal strip.

Again, fix $\alpha, \beta \in \Lambda_{d,\ell}$, and now let $T \in \mathrm{SSCT}_{d,\ell}(\alpha/\mu)$ and $U \in \mathrm{SSCT}_{d,\ell}(\beta/\mu)$, where $\mu \subseteq \alpha, \beta$. Let N and M be upper bounds on the entries of T and U, respectively. To compute $(P, Q) = \mathrm{CRSK}(T, U)$, we will build a cylindric growth diagram on a $M \times N$ rectangular grid, where again each vertex is labeled with an element of $\Lambda_{d,\ell}$.

We start by labeling the vertices in the left boundary of the grid, from bottom to top, by the sequence $\mathrm{ssh}(T)$, and the vertices in the bottom boundary, from left to right, by the sequence $\mathrm{ssh}(U)$. See Figure 2 for an example.

The forward local rule that computes $\rho^{\urcorner}$ given the labels $\rho^{\llcorner}$, $\rho^{\ulcorner}$ and $\rho^{\lrcorner}$ of the vertices of a unit square, as in the diagram (3.1), is now generalized by letting

$$\rho^{\urcorner}_i = \max\{\rho^{\ulcorner}_i, \rho^{\lrcorner}_i\} + \min\{\rho^{\ulcorner}_{i-1}, \rho^{\lrcorner}_{i-1}\} - \rho^{\llcorner}_{i-1} \tag{3.2}$$

for all i. It is not hard to see that this rule restricts to (F1) and (F2) when both $\rho^{\ulcorner}$ and $\rho^{\lrcorner}$ are obtained from $\rho^{\llcorner}$ by adding one cell.

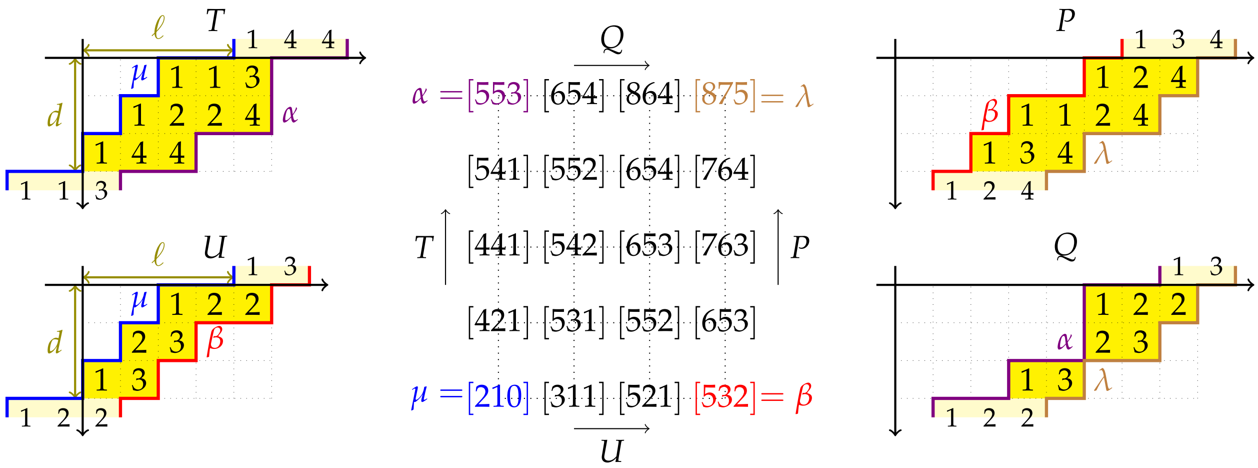

Figure 2: The computation of $\mathrm{CRSK}(T,U) = (P,Q)$ using growth diagrams.

As an example of equation (3.2), let $\rho^{\llcorner} = [2,1,0]$, $\rho^{\ulcorner} = [4,2,1]$ and $\rho^{\lrcorner} = [3,1,1]$, as in the bottom-left square in Figure 2. Then $\rho^{\urcorner}_1 = \max\{4,3\} + \min\{5,5\} - 4 = 5$, $\rho^{\urcorner}_2 = \max\{2,1\} + \min\{4,3\} - 2 = 3$ and $\rho^{\urcorner}_3 = \max\{1,1\} + \min\{2,1\} - 1 = 1$, so $\rho^{\urcorner} = [5,3,1]$.

The next lemma shows that the forward local rule (3.2) has the desired properties when applied to horizontal strips.

Lemma 2. *Suppose that $\rho^{\llcorner}, \rho^{\ulcorner}, \rho^{\llcorner}, \rho^{\urcorner} \in \Lambda_{d,\ell}$ satisfy equation (3.2). Then $\rho^{\ulcorner}/\rho^{\llcorner}$ and $\rho^{\lrcorner}/\rho^{\llcorner}$ are horizontal strips if and only if so are $\rho^{\urcorner}/\rho^{\lrcorner}$ and $\rho^{\urcorner}/\rho^{\ulcorner}$. In addition, $|\rho^{\urcorner}/\rho^{\lrcorner}| = |\rho^{\ulcorner}/\rho^{\llcorner}|$ and $|\rho^{\urcorner}/\rho^{\ulcorner}| = |\rho^{\lrcorner}/\rho^{\llcorner}|$.*

Once all the labels of the grid have been computed, let λ be the label of vertex (M,N). Let $P \in \mathrm{SSCT}_{d,\ell}(\lambda/\beta)$ be determined by the sequence of the labels of the right boundary of the grid, and let $Q \in \mathrm{SSCT}_{d,\ell}(\lambda/\alpha)$ be determined by the sequence of labels of the top boundary. Lemma 2 guarantees that P and Q are semistandard cylindric tableaux, and that $\mathrm{wt}(P) = \mathrm{wt}(T)$ and $\mathrm{wt}(Q) = \mathrm{wt}(U)$.

In these growth diagrams for SSCT, the backward rule to compute $\rho^{\llcorner}$ given $\rho^{\ulcorner}$, $\rho^{\lrcorner}$ and $\rho^{\urcorner}$ is obtained by solving equation (3.2) for $\rho^{\llcorner}_{i-1}$ and shifting the indices:

$$\rho^{\llcorner}_i = \max\{\rho^{\ulcorner}_{i+1}, \rho^{\lrcorner}_{i+1}\} + \min\{\rho^{\ulcorner}_i, \rho^{\lrcorner}_i\} - \rho^{\urcorner}_{i+1}$$

for all i.

An alternative way to compute growth diagrams is by labeling each edge by the difference of the labels of its endpoints. Specifically, for a square with vertex labels as in equation (3.1), we label the top, bottom, left and right edges by $\delta^T = \rho^{\urcorner} - \rho^{\ulcorner}$, $\delta^B = \rho^{\lrcorner} - \rho^{\llcorner}$, $\delta^L = \rho^{\ulcorner} - \rho^{\llcorner}$ and $\delta^L = \rho^{\ulcorner} - \rho^{\llcorner}$, respectively. Then we can translate equation (3.2) into a rule to compute δ^R and δ^T in terms of δ^L and δ^B. Specifically, if we let $m_i = \min\{\delta^L_i, \delta^B_i\}$ and $\Delta m_i = m_{i-1} - m_i$ for all i, then we have $\delta^R = \delta^L + \Delta m$ and

$\delta^T = \delta^B + \Delta m$. For example, if $\delta^L = [2,1,1]$ and $\delta^B = [1,0,1]$, then $m = [1,0,1]$ and $\Delta m = [0,1,-1]$, so $\delta^T = [1,0,1] + [0,1,-1] = [1,1,0]$ and $\delta^R = [2,1,1] + [0,1,-1] = [2,2,0]$.

3.3 Properties

One advantage of the growth diagram description of CRSK is that it explains the symmetry of this correspondence when T and U are swapped. The following result was proved by Neyman [12] using the insertion description, adapting a similar result for skew tableaux [16, Thm. 3.3]. We can now provide a more transparent proof.

Corollary 3 ([12, Thm. 5.18])**.** *If* $\mathrm{CRSK}(T,U) = (P,Q)$*, then* $\mathrm{CRSK}(U,T) = (Q,P)$.

Proof. The local rule in equation (3.2) is symmetric with respect to switching the axes, since it does not distinguish between $\rho^{\ulcorner}$ and $\rho^{\lrcorner}$. Thus, the growth diagram for the pair (U,T) is the reflection of the growth diagram for the pair (T,U). This reflection swaps the upper boundary with the right boundary, and hence the roles of P and Q. □

A different property of CRSK concerns a complementation operation on cylindric tableaux. For a cylindric shape $\lambda = [\lambda_1, \lambda_2, \ldots, \lambda_d] \in \Lambda_{d,\ell}$, let $\bar{\lambda} = [\ell - \lambda_d, \ell - \lambda_{d-1}, \ldots, \ell - \lambda_1] \in \Lambda_{d,\ell}$. For $T \in \mathrm{SSCT}(\lambda/\mu)$ with smallest entry 1 and largest entry N, define its *complement* to be the tableau $\overline{T} \in \mathrm{SSCT}_{d,L}(\bar{\mu}/\bar{\lambda})$ such that $\overline{T}(\langle d+1-i, \ell+1-j\rangle) = N + 1 - T(\langle i,j\rangle)$ for all $\langle i,j\rangle \in Y_{\lambda/\mu}$. In other words, $\overline{T}$ is obtained from T by performing a 180° rotation and replacing each entry k with $N+1-k$.

The following property of CRSK was first proved by Neyman [12]. Cylindric growth diagrams provide a simpler proof. Indeed, rotating by 180° the cylindric growth diagram that computes $\mathrm{CRSK}(T,U) = (P,Q)$ and replacing each label ρ with $\bar{\rho}$ yields the cylindric growth diagram that computes $\mathrm{CRSK}(\overline{P},\overline{Q}) = (\overline{T},\overline{U})$.

Corollary 4 ([12, Cor. 4.19])**.** *If* $\mathrm{CRSK}(T,U) = (P,Q)$*, then* $\mathrm{CRSK}(\overline{P},\overline{Q}) = (\overline{T},\overline{U})$.

4 Walks in simplices and oscillating cylindric tableaux

4.1 Walks in a simplicial region

In [11], Mortimer and Prellberg studied lattice walks in the region

$$\Delta_{d,\ell} = \{(x_1, x_2, \ldots, x_d) \in \{0,1,2,\ldots\}^d : x_1 + x_2 + \cdots + x_d = \ell\}$$

with steps $s_i = e_{i+1} - e_i$ and $\bar{s}_i = e_i - e_{i+1}$ for $1 \le i \le d$, where the e_i are the coordinate vectors, and indices are taken modulo d. See Figure 3 for an example on a walk in $\Delta_{3,2}$. Using the kernel method, they enumerated n-step walks starting at a given $\mathbf{x} \in \Delta_{d,\ell}$ in

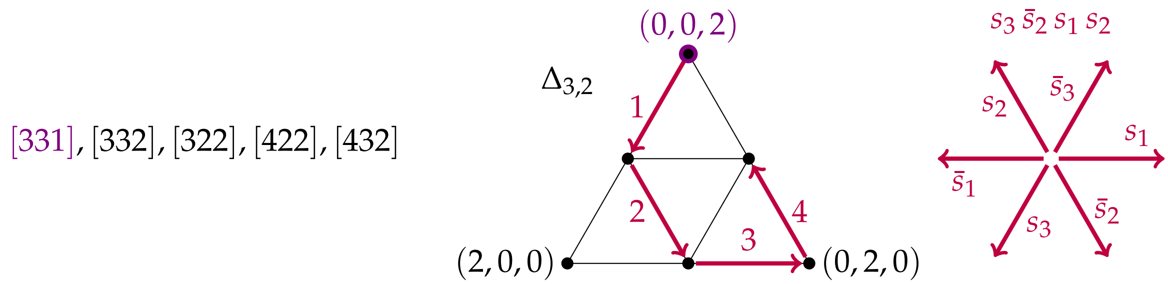

Figure 3: An oscillating cylindric tableau in $\mathrm{OCT}_{3,2}(\alpha/\cdot)$ and the corresponding walk in $\mathcal{W}_{3,2}(\mathbf{x})$, where $\alpha = [3,3,1] \in \Lambda_{3,2}$ and $\mathbf{x} = (0,0,2) \in \Delta_{3,2}$.

the case $d = 3$. When $\mathbf{x} = (\ell, 0, 0)$, they found a surprising connection to Motzkin paths of bounded height.

This connection was later explained bijectively by Courtiel et al. [2], who, in the process, proved the following theorem about such walks. Let the type of an n-step walk be the word $w \in \{+,-\}^n$ whose kth entry is $+$ or $-$ if the kth step of the walk is of the form s_i of $\bar{s}_i$, respectively. Let $\mathcal{W}^w_{d,\ell}(\mathbf{x})$ be the set of walks of type w starting at $\mathbf{x}$.

Theorem 5 ([2, Thm. 6 & 34])**.** *Let $\mathbf{x} \in \Delta_{d,\ell}$ and $n \geq 0$. For any $w, w' \in \{+,-\}^n$, there is a bijection between $\mathcal{W}^w_{d,\ell}(\mathbf{x})$ and $\mathcal{W}^{w'}_{d,\ell}(\mathbf{x})$.*

The proof given in [2] repeatedly applies certain flips to adjacent steps and to the last step of a walk of type w starting at $\mathbf{x}$ until it becomes a walk of type w'. An alternative description of this construction is given in [2, Sec. 2.3] in terms of tilings of a tilted square with labeled tiles that must follow certain rules that emulate the allowed flips in the walks. The authors then use induction to prove that the tiling exists and is unique.

Let us show that cylindric growth diagrams can be used to provide a more natural proof of Theorem 5.

4.2 Oscillating cylindric tableaux

In analogy with the notion of oscillating tableaux [14, 9], we define *oscillating cylindric tableaux* to be sequences $\rho^0, \rho^1, \dots, \rho^n$ of cylindric shapes in $\Lambda_{d,\ell}$ where each shape is obtained from the previous one by either adding or removing one cell.

The type of an oscillating cylindric tableau is the word in $\{+,-\}^n$ whose kth entry is $+$ if $\rho^{k-1} \subset \rho^k$, and $-$ if $\rho^{k-1} \supset \rho^k$, for $1 \leq k \leq n$. Oscillating cylindric tableau of type $+^n$ can be identified with standard cylindric tableaux with n cells via the correspondence $T \mapsto \mathrm{ssh}(T)$ defined in equation (2.1). For $\alpha \in \Lambda_{d,\ell}$ and $w \in \{+,-\}^n$, let $\mathrm{OCT}^w_{d,\ell}(\alpha,\cdot)$ denote the set of oscillating cylindric tableaux $\rho^0, \rho^1, \dots, \rho^n$ of type w where $\rho^0 = \alpha$.

It is shown in [3] that there is a simple bijection between $\mathrm{OCT}^{w}_{d,\ell}(\alpha,\cdot)$ and $\mathcal{W}^{w}_{d,\ell}(\mathbf{x})$, where $\mathbf{x} = (x_1, x_2, \ldots, x_d) \in \Delta_{d,\ell}$ has coordinates $x_i = \alpha_{i-1} - \alpha_i$ for $1 \leq i \leq d$. See Figure 3 for an example. This allows us to reformulate Theorem 5 as a statement about oscillating cylindric tableaux. Then, by interpreting oscillating cylindric tableaux as paths with east and south steps along the edges of cylindric growth diagrams, we can prove the next result (see [3] for details), from where Theorem 5 follows. We say that a cylindric growth diagram is symmetric if it is invariant under reflection along $y = x$.

Theorem 6. *Let $\alpha \in \Lambda_{d,\ell}$ and $w \in \{+,-\}^n$ for some $n \geq 0$. There is a bijection between $\mathrm{OCT}^{w}_{d,\ell}(\alpha,\cdot)$ and the set of symmetric cylindric growth diagrams for SCT on an $n \times n$ grid where vertices $(0,n)$ and $(n,0)$ have label α. In particular, for any $w, w' \in \{+,-\}^n$, there is a bijection between $\mathrm{OCT}^{w}_{d,\ell}(\alpha,\cdot)$ and $\mathrm{OCT}^{w'}_{d,\ell}(\alpha,\cdot)$.*

Even though there is no mention of growth diagrams or cylindric tableaux in [2], one can argue that the tiles essentially simulate the local rules of cylindric growth diagrams for SCT. In particular, if one generalizes the tiling from [2, Sec. 2.3] to arbitrary d, the resulting bijection, when translated to a bijection from $\mathcal{O}^{w}_{d,\ell}(\mathbf{x})$ to $\mathcal{O}^{w'}_{d,\ell}(\mathbf{x})$, is equivalent to the one that we obtain in our proof of Theorem 6 using cylindric growth diagrams.

4.3 Further directions

Huh, Kim, Krattenthaler and Okada [7] have recently found a surprising connection between standard cylindric tableaux and certain matchings. In our notation, letting $[0^d] = [0, \ldots, 0] \in \Delta_{d,\ell}$, they prove in [7, Cor. 8.9] that $\left|\mathrm{SCT}^{n}_{d,\ell}(\cdot/[0^d])\right|$ equals the number of partial matchings on n points avoiding certain generalized crossings and nestings. Their proofs are computational, based on explicit determinantal formulas. Bijections are known only in very specific cases, when $d \leq 3$ or $d \to \infty$. We wonder if the cylindric growth diagrams that we introduced here, or some generalization of them, might be helpful in finding a general bijection between standard cylindric tableaux and restricted partial matchings.

In a different direction, one could ask if some parts of the theory of r-differential posets [17] can be adapted to the poset $(\Lambda_{d,\ell}, \subseteq)$ of cylindric shapes ordered by containment, which is not an r-differential poset in the sense of [17, Def. 1.1], but it has similar properties if we allow $r = 0$ and do not require the poset to have a minimal element. In this case, the analogous linear transformations U and D on the vector space of linear combinations of elements of $\Lambda_{d,\ell}$ commute.

Acknowledgments

The author thanks Alex Postnikov, Darij Grinberg and Christian Krattenthaler for helpful conversations about cylindric tableaux and growth diagrams. This work was partially supported by Simons Collaboration Grant #929653.

References

[1] A. Berenstein and A. N. Kirillov. "The Robinson–Schensted–Knuth bijection, quantum matrices and piece-wise linear combinatorics". Proceedings of FPSAC 2001. 2001. Link.

[2] J. Courtiel, A. Elvey Price, and I. Marcovici. "Bijections between walks inside a triangular domain and Motzkin paths of bounded amplitude". *Electron. J. Combin.* **28**.2 (2021), Paper No. 2.6, 44. DOI.

[3] S. Elizalde. "Cylindric growth diagrams, walks in simplices, and exclusion processes". Preprint. 2025. arXiv:2507.01097. Link.

[4] S. V. Fomin. "The generalized Robinson-Schensted-Knuth correspondence". *Zap. Nauchn. Sem. Leningrad. Otdel. Mat. Inst. Steklov. (LOMI)* **155** (1986), pp. 156–175, 195. DOI.

[5] S. Fomin. "Schensted algorithms for dual graded graphs". *J. Algebraic Combin.* **4**.1 (1995), pp. 5–45. DOI.

[6] I. M. Gessel and C. Krattenthaler. "Cylindric partitions". *Trans. Amer. Math. Soc.* **349**.2 (1997), pp. 429–479. DOI.

[7] J. Huh, J. S. Kim, C. Krattenthaler, and S. Okada. "Bounded Littlewood identities for cylindric Schur functions". *Trans. Amer. Math. Soc.* **378**.10 (2025), pp. 6765–6829. DOI.

[8] C. Krattenthaler. "Growth diagrams, and increasing and decreasing chains in fillings of Ferrers shapes". *Adv. in Appl. Math.* **37**.3 (2006), pp. 404–431. DOI.

[9] C. Krattenthaler. "Bijections between oscillating tableaux and (semi)standard tableaux via growth diagrams". *J. Combin. Theory Ser. A* **144** (2016), pp. 277–291. DOI.

[10] P. McNamara. "Cylindric skew Schur functions". *Adv. Math.* **205**.1 (2006), pp. 275–312. DOI.

[11] P. R. G. Mortimer and T. Prellberg. "On the number of walks in a triangular domain". *Electron. J. Combin.* **22**.1 (2015), Paper 1.64, 15. Link.

[12] E. Neyman. "Cylindric Young Tableaux and their Properties". 2015. arXiv:1410.5039. Link.

[13] A. Postnikov. "Affine approach to quantum Schubert calculus". *Duke Math. J.* **128**.3 (2005), pp. 473–509. DOI.

[14] T. W. Roby. "Applications and extensions of Fomin's generalization of the Robinson-Schensted correspondence to differential posets". Thesis. Massachusetts Institute of Technology, 1991. Link.

[15] B. E. Sagan. *The symmetric group*. Second. Vol. 203. Graduate Texts in Mathematics. Springer-Verlag, New York, 2001. DOI.

[16] B. E. Sagan and R. P. Stanley. "Robinson-Schensted algorithms for skew tableaux". *J. Combin. Theory Ser. A* **55**.2 (1990), pp. 161–193. DOI.

[17] R. P. Stanley. "Differential posets". *J. Amer. Math. Soc.* **1**.4 (1988), pp. 919–961. DOI.

[18] R. P. Stanley. *Enumerative combinatorics. Vol. 2*. Vol. 62. Cambridge Studies in Advanced Mathematics. Cambridge University Press, Cambridge, 1999. DOI.